Experimental investigation of interface states and photovoltaic effects on the scanning capacitance microscopy measurement for *p-n* junction dopant profiling

J. Yang[a)]
School of Information Technology and Electrical Engineering, The University of Queensland, St. Lucia, Australia 4072

J. J. Kopanski
Semiconductor Electronics Division, National Institute of Standards and Technology, Gaithersburg, Maryland 20899-8120

A. Postula and M. Bialkowski
School of Information Technology and Electrical Engineering, The University of Queensland, St. Lucia, Australia 4072

(Received 7 October 2004; accepted 16 March 2005; published online 25 April 2005)

Controlled polishing procedures were used to produce both uniformly doped and *p-n* junction silicon samples with different interface state densities but identical oxide thicknesses. Using these samples, the effects of interface states on scanning capacitance microscopy (SCM) measurements could be singled out. SCM measurements on the junction samples were performed with and without illumination from the atomic force microscopy laser. Both the interface charges and the illumination were seen to affect the SCM signal near *p-n* junctions significantly. SCM *p-n* junction dopant profiling can be achieved by avoiding or correctly modeling these two factors in the experiment and in the simulation. © *2005 American Institute of Physics*. [DOI: 10.1063/1.1922077]

The *International Technology Roadmap for Semiconductors* predicted requirements for two-dimensional (2-D) quantitative dopant profiling are for a 2 nm spatial resolution and 2% accuracy by 2016.[1] Scanning capacitance microscopy (SCM) has the potential to fulfill these requirements. SCM detects the differential capacitance dC/dV of the metal-oxide-semiconductor (MOS) structure formed by the SCM tip, a surface oxide layer, and an underlying semiconductor sample. Since the dC/dV is inversely related to the dopant concentration in the semiconductor, it is possible to extract the dopant concentration from the SCM signals. In recent years, SCM models based on the conventional one-dimensional (1-D) analytic solution of the MOS capacitance-voltage (*C-V*) characteristics have been used to extract 2-D carrier profiles in unipolar samples.[2–5] At the same time, scanning capacitance spectroscopy, a variant of SCM, has been used to delineate *p-n* junctions in silicon transistor cross-sections.[6–8] More recent developments related to SCM dopant profiling include: the improvement of the spatial resolution by reducing the tip size[9] or using beveled samples;[10,11] the improved understanding of the impacts of interface charges[12–16] and atomic force microscopy (AFM) laser[17–19] on SCM measurements; and the improvement of the data interpretation techniques.[20] However, SCM dopant profiling across *p-n* junctions has not been fully achieved because the interpretation of SCM signals of *p-n* junctions still remains a challenge.[5,8]

It is well known that the SCM *C-V* curves become "U" shaped when the SCM tip is approaching a junction. This is because, when the tip is close enough to the junction (theoretically speaking, within one diffusion length of the minority carriers), the majority carriers in the opposite side of the junction induced by the tip fringing field are able to travel to the inversion region beneath the tip. As a result, holes and electrons will accumulate alternatively beneath the tip when the sample/tip dc bias V_{dc} is swept from the positive to the negative, giving the "U" shaped *C-V* curves. This is a three-dimensional phenomenon that cannot be explained by the above-mentioned 1-D analytic models. To pursue the SCM dopant profiling of *p-n* junctions, we recently proposed a different approach through comparison of 2-D numerical simulations and the measured peak dC/dV signal as a function of x (the tip position across the junction) profile.[21] However, there was a discrepancy between the simulation and the experimental peak dC/dV profile in the vicinity of the junction. Our further simulation suggested that this discrepancy may be caused by the interface states; i.e., the interface states with an amphoteric energy distribution may depress the magnitude of the peak dC/dV signal near the *p-n* junction.[13] More recently, we presented an experimental investigation for this interface states effect.[16] A special sample preparation method was used to make samples with different interface state densities and an identical oxide thickness. That is, diamond and colloidal silica suspensions of different particle sizes were used at the final step of the polish process to create different surface damages on the samples, followed by an identical low-temperature oxidation process. By comparing SCM signals of these samples, the effect of interface states has been singled out. However, until now, all the experimental investigation of the interface states effect have been conducted on unipolar samples.[12,14–16] Moreover, it has recently become clear that the stray light from the atomic force microscope (AFM) laser can drastically affect the SCM signal, because it generates local nonequilibrium carriers (the photovoltaic effect).[17–19] The dC/dV signal in the vicinity of *p-n* junctions should be more vulnerable to the illumination due to the low concentration of equilibrium free carriers in

[a)]Electronic mail: yjaus2002@yahoo.com

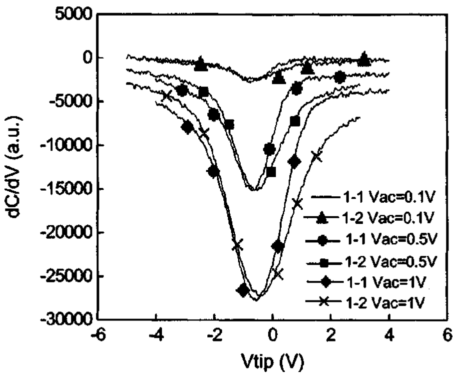

FIG. 1. Experimental $dC/dV-V_{\mathrm{tip}}$ data of samples 1-1 and 1-2 measured with three different values of V_{ac} (0.1, 0.5, and 1 V) and a V_{ac} frequency of 20 kHz in the true dark condition.

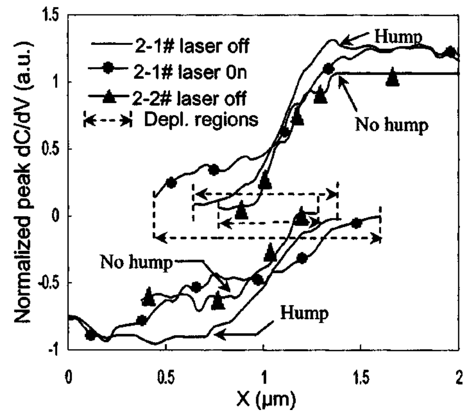

FIG. 2. The experimental peak dC/dV-x data of sample 2-1 obtained with laser off and on, and of sample 2-2 obtained with laser off.

this region. Consequently, the interface states and the photovoltaic effects have to be well understood in order to extract dopant profiles of *p-n* junctions.

In this work, the interface states and photovoltaic effects on SCM signals near *p-n* junctions are experimentally investigated. Improvements for the extraction of *p-n* junction dopant profile based on the understanding of these two important effects are also presented.

For the clarity of this letter, we repeat part of the previous experiment on the unipolar samples first. Samples 1-1 and 1-2 were polished using 0.02 μm colloidal silica and 0.25 μm diamond suspensions, giving rms surface roughness of 0.233 and 0.482 nm, respectively. Sample 1-2 is supposed to have high interface states density because greater surface roughness contributes more silicon dangling bond defects on the sample surfaces, resulting in higher interface state densities after oxidation. These two samples were cut from the same (100) *p*-type wafer with a uniform dopant concentration of 1×10^{16} cm^{-3}. Both samples were cleaned with UV-generated ozone for 20 min, followed by a 300 °C oxidation in 5% ozone/95% oxygen for 2 h, giving an oxide thickness of about 4 nm.[22] Figure 1 shows the $dC/dV-V_{\mathrm{tip}}$ ($V_{\mathrm{tip}}=-V_{\mathrm{dc}}$) curves of samples 1-1 and 1-2 measured with different amplitudes (0.1, 0.5, and 1 V) of the sample/tip ac bias V_{ac}, at a frequency of 20 kHz and with the AFM laser off. The results show that the peak dC/dV values of these two samples are nearly the same for all the three V_{ac} values. At the same time, the full width at half-maximum values of sample 1-2 are bigger than those of sample 1-1, indicating that the sample preparation method is able to incorporate higher interface states density in sample 1-2.[12,16] These results lead to a conclusion that the magnitude of the peak dC/dV is independent of interface states.

To investigate the interface states and the photovoltaic effects on the SCM signals near *p-n* junctions, two n/p^+ junction samples were prepared using the above-mentioned method (i.e., 0.02 μm colloidal silica for sample 2-1 and 0.5 μm diamond slurry for sample 2-2). The junction in these two samples is formed by a *n*-type epitaxial layer (uniformly doped at 4.6×10^{15} cm^{-3}, 12.2 μm thickness) and a (110) p^+ silicon substrate (uniformly doped at 2.3 $\times10^{18}$ cm^{-3}). Sample 2-2 has a slightly thicker oxide than sample 2-1. However, based on the above results for samples 1-1 and 1-2, we believe the peak dC/dV values in the neutral regions of these two samples would be the same if the oxide thicknesses of the two samples were identical. Thus, we can normalize the dC/dV data using the peak dC/dV values in the *n*-type neutral regions.

We measured the peak dC/dV-x data of samples 2-1 and 2-2 with the laser on the SCM tip and in the true dark (laser off) conditions. When the AFM laser is turned off, the feedback loop of the cantilever deflection detection circuit will continue to adjust the driving voltage of the microscope piezoelectric scanner in the vertical direction attempting to maintain a constant laser reflection. This may shift the tip position between when the laser is on and when the laser is switched off. To ensure the accuracy of the tip position detection, we set the "deflection setpoint" in the feedback controls equal to zero in experiment and performed the measurement of the $dC/dV-V_{\mathrm{dc}}$ curve with a loop of three steps; i.e., with the laser on, the laser off, and the laser on again. Only if the dC/dV characteristics obtained with the laser-on and the laser-on-again were identical with each other were the data accepted and the tip shifted to the next point to continue the measurement. Using this approach, the $dC/dV-V_{\mathrm{dc}}$ curves were obtained as the tip scanned across the junctions in spatial intervals of 0.05 μm. The peak dC/dV values were then obtained from each $dC/dV-V_{\mathrm{dc}}$ curve to produce the peak dC/dV-x profile. Note that, the *C-V* curve of neutral regions takes a shape like a conventional high-frequency *C* -*V* curve, giving one peak dC/dV value (positive value for *n*-type and negative for *p*-type region) and when the tip rests in the depletion region near the junction, the "U" shaped *C* -*V* curve gives two peak dC/dV values (one positive and one negative). Thus, the positive and the negative peak dC/dV -x curves overlap in the measured depletion region.

Figure 2 shows the normalized peak dC/dV-x results of sample 2-1 obtained with the laser on (solid circles) and off (solid line); and the normalized peak dC/dV-x data of sample 2-2 obtained with the laser off (solid triangles). A comparison of the two curves of sample 2-1 in Fig. 2 reveals two effects of the illumination. Firstly, the measured depletion region (or the peak dC/dV overlapping region) is broadened by the illumination. Secondly, there are increases in magnitude (humps) in the peak dC/dV signal on both sides of the depletion region in the data measured in the dark as compared to the data obtained with the laser on. Both of these two effects can be attributed to the laser generated excess nonequilibrium carriers. That is, when the laser is on, the quantity and the recombination lifetime of free carriers will increase. As a result, the carriers are able to cover a longer distance across the junction, making the measured

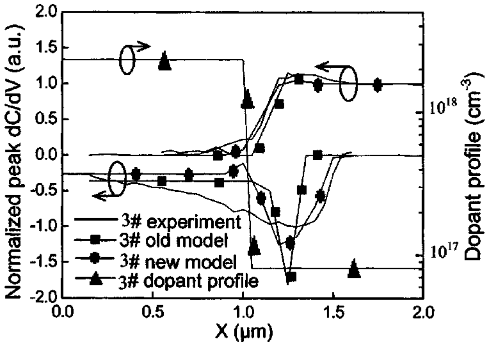

FIG. 3. The result of dopant profile extraction of a *p-n* junction (sample 3) using experimental data obtained from a sample of fine surface polish under the true dark condition and the 2-D numerical simulation models.

depletion region wider. On the other hand, under the true dark condition, the concentration of free carriers in the depletion region of the *p-n* junction is lower compared to that in the neutral regions, resulting in bigger values of the peak dC/dV signal. Note that in Fig. 2, as well as in the following Fig. 3, the central positions of the overlapping regions are used as the position reference to align all the dC/dV-x curves along the x axis.

Comparison of the two peak dC/dV-x curves (laser off) of samples 2-1 and 2-2 in Fig. 2 reveals the effect of interface states. Two differences between these two curves can be observed. The first is that the measured depletion region of sample 2-2, which is supposed to have the higher interface states density, is narrower than that of sample 2-1. This can be attributed to the decrease of the minority lifetime and the carrier mobility at the silicon surface with the increase of the interface defects. The other difference is that there are no apparent humps in the peak dC/dV-x curve of sample 2-2 as compared to that of sample 2-1. This validates our earlier simulation results, which show the interface states depress the peak dC/dV values near *p-n* junctions.[13]

Interface states and the photovoltaic effect both deteriorate the detection of the SCM signal, especially near *p-n* junctions. Thus, for the *p-n* junction dopant profiling, experimental data acquired with the true dark condition using samples of low interface charge density are necessary. Figure 3 shows a result of dopant profile extraction of a junction using this approach. The junction is a *n*-type epitaxial layer (uniformly doped at 8.07×10^{16} cm^{-3}, 11.1 μm thickness) on a (110) p^+ silicon substrate (uniformly doped at 2.3 $\times10^{18}$ cm^{-3}). This sample (sample 3) is used here because, compared to sample 2-1, the experimental peak dC/dV profile of this sample covers full region of the junction with the same measuring distance (2 μm) due to the narrower depletion region (or the higher dopant concentration). The sample surface was polished using 0.02 μm colloidal silica to decrease the surface roughness. A new model improved from our earlier model[13] was used for this simulation. This is because the earlier model gave a narrower simulated overlapping region (solid squares in Fig. 3) compared to the experimental peak dC/dV profile (solid line), which can be attributed to that the fringing field around the tip in the earlier model is too small compared to what in practice. In our model, a round tip shape (radius=0.2 μm) and a higher dielectric constant ($\varepsilon=8$) in the region of air are specified to increase the fringing field around the tip. The new model has no allowance for interface states at this stage. Figure 3 shows that the simulation result of the new model (solid circles) and the experimental peak dC/dV profile, corresponding to the same dopant profile (solid triangles), qualitatively match with each other. This result, plus our earlier simulation work of the SCM interface states model,[13] leads to a conclusion that the SCM dopant profiling of a *p-n* junction is achievable after taking into account the interface states and the photovoltaic effects in the experiment and in the simulation. The details of this simulation work will be published elsewhere.

This work was partially supported by the Graduate School Research Travel Award (GSRTA) of the University of Queensland, Australia, and also by the National Semiconductor Metrology Program at National Institute of Standards and Technology (NIST), USA. Details of all the experiment facilities used in this work can be found in another publication.[23]

[1] *International Technology Roadmap for Semiconductors* (European Semiconductor Industry Association, Japan Electronics and Information Technology Industries Association, Korea Semiconductor Industry Association, and Taiwan Semiconductor Industry Association, and the Semiconductor Industry Association, San Jose, CA, 2003).
[2] Y. Huang, C. C. Williams, and H. Smith, J. Vac. Sci. Technol. B **14**, 433 (1996).
[3] J. S. McMurray, J. Kim, and C. C. Williams, J. Vac. Sci. Technol. B **15**, 1011 (1997).
[4] J. J. Kopanski, J. F. Marchiando, D. W. Berning, R. Alvis, and H. E. Smith, J. Vac. Sci. Technol. B **16**, 339 (1998).
[5] B. G. Rennex, J. J. Kopanski, and J. F. Marchiando, Proc. Intern. Conf. Charac. and Metro. for ULSI Tech., 2000, p. 635.
[6] C. J. Kang, C. K. Kim, J. D. Lera, Y. Kuk, K. M. Mang, J. G. Lee, K. S. Suh, and C. C. Williams, Appl. Phys. Lett. **71**, 1546 (1997).
[7] H. Edwards, R. McGlothlin, R. S. Martin, E. U. M. Gribelyuk, R. Mahaffy, C. K. Shih, R. S. List, and V. A. Ukraintsev, Appl. Phys. Lett. **72**, 698 (1998).
[8] V. V. Zavyalov, J. S. McMurray, and C. C. Williams, J. Appl. Phys. **85**, 7774 (1999).
[9] E. Bussmann and C. C. Williams, Rev. Sci. Instrum. **75**, 422 (2004).
[10] F. Giannazzo, F. Priolo, V. Raineri, and V. Privitera, Appl. Phys. Lett. **76**, 2565 (2000).
[11] N. Duhayon, T. Clarysse, P. Eyben, W. Vandervorst, and L. Hellemans, J. Vac. Sci. Technol. B **20**, 741 (2002).
[12] O. Bowallius and S. Anand, Mater. Sci. Semicond. Process. **4**, 81 (2001).
[13] J. Yang and F. C. J. Kong, Appl. Phys. Lett. **81**, 4973 (2002).
[14] W. K. Chim, K. M. Wong, Y. T. Yeow, Y. D. Hong, Y. Lei, L. W. Teo, and W. K. Choi, IEEE Electron Device Lett. **24**, 667 (2003).
[15] J. J. Kopanski, W. R. Thurber, and M. L. Chun (unpublished).
[16] J. Yang, J. J. Kopanski, A. Postula, and M. Bialkowski, Microelectron. Reliab. **45**, 887 (2005).
[17] S. Shin, J.-I. Kye, U. H. Pi, Z. G. Khim, J. W. Hong, S.-I. Park, and S. Yoon, J. Vac. Sci. Technol. B **18**, 2664 (2000).
[18] M. N. Chang, C. Y. Chen, F. M. Pan, J. H. Lai, W. W. Wan, and J. H. Liang, Appl. Phys. Lett. **82**, 3955 (2003).
[19] G. H. Buh and J. J. Kopanski, Appl. Phys. Lett. **83**, 2486 (2003).
[20] J. F. Marchiando and J. J. Kopanski, J. Appl. Phys. **92**, 5798 (2002).
[21] J. Yang, Y. T. Yeow, J. J. Kopanski, and W. K. Chim (unpublished).
[22] J. Y. Zhang and I. W. Boyd, Electron. Lett. **32**, 2097 (1996).
[23] J. J. Kopanski, J. F. Marchiando, and B. G. Rennex, J. Vac. Sci. Technol. B **20**, 2101 (2002).